Video Article

Visualizing and Analyzing Intracellular Transport of Organelles and Other Cargos in Astrocytes

Blake A. Creighton*[1], Theodore W. Ruffins*[1], Damaris N. Lorenzo[1]

[1]Department of Cell Biology and Physiology, University of North Carolina at Chapel Hill

*These authors contributed equally

Correspondence to: Damaris N. Lorenzo at damaris_lorenzo@med.unc.edu

URL: https://www.jove.com/video/60230
DOI: doi:10.3791/60230

Keywords: Neuroscience, Issue 150, astrocytes, intracellular transport, live-imaging, trafficking kinetics, degradative endosomes, connexin 43, EAAT1

Date Published: 8/28/2019

Citation: Creighton, B.A., Ruffins, T.W., Lorenzo, D.N. Visualizing and Analyzing Intracellular Transport of Organelles and Other Cargos in Astrocytes. *J. Vis. Exp.* (150), e60230, doi:10.3791/60230 (2019).

Abstract

Astrocytes are among the most abundant cell types in the adult brain, where they play key roles in a multiplicity of functions. As a central player in brain homeostasis, astrocytes supply neurons with vital metabolites and buffer extracellular water, ions, and glutamate. An integral component of the “tri-partite” synapse, astrocytes are also critical in the formation, pruning, maintenance, and modulation of synapses. To enable these highly interactive functions, astrocytes communicate among themselves and with other glial cells, neurons, the brain vasculature, and the extracellular environment through a multitude of specialized membrane proteins that include cell adhesion molecules, aquaporins, ion channels, neurotransmitter transporters, and gap junction molecules. To support this dynamic flux, astrocytes, like neurons, rely on tightly coordinated and efficient intracellular transport. Unlike neurons, where intracellular trafficking has been extensively delineated, microtubule-based transport in astrocytes has been less studied. Nonetheless, exo- and endocytic trafficking of cell membrane proteins and intracellular organelle transport orchestrates astrocytes’ normal biology, and these processes are often affected in disease or in response to injury. Here we present a straightforward protocol to culture high quality murine astrocytes, to fluorescently label astrocytic proteins and organelles of interest, and to record their intracellular transport dynamics using time-lapse confocal microscopy. We also demonstrate how to extract and quantify relevant transport parameters from the acquired movies using available image analysis software (i.e., ImageJ/FIJI) plugins.

Video Link

The video component of this article can be found at https://www.jove.com/video/60230/

Introduction

Astrocytes are the most abundant cells in the adult central nervous system, where they perform unique developmental and homeostatic functions[1]. Astrocytes modulate synaptic development through direct contact with pre- and postsynaptic terminals as part of the tri-partite synapse, which contains neurotransmitter receptors, transporters, and cell adhesion molecules that facilitate synapse formation and neuron-astrocyte communication[2]. In addition, astrocytes actively control synaptic transmission and prevent neuronal excitotoxicity by rapidly removing excitatory neurotransmitters from the synaptic cleft, recycling neurotransmitters, and participating in synaptic pruning[3,4,5,6]. To enable these highly interactive functions, astrocytes communicate among themselves, with other glial cells, and with neurons through specialized membrane proteins, including cell adhesion molecules, aquaporins, ion channels, neurotransmitter transporters, and gap junction molecules. Astrocytes actively change the surface levels of these proteins in response to fluctuations in their intra- and extracellular environment[7]. Furthermore, changes in the levels and distribution of mitochondria, lipid droplets, and degradative and recycling organelles modulate energy supply, metabolite availability, and cellular clearing processes that are essential for astrocyte function and survival.

The dynamic changes in membrane protein and organelle trafficking and positioning in astrocytes are facilitated by the concerted function of motor proteins and adaptors that promote cargo motility[8,9]. Similarly, surface levels of membrane proteins are modulated through internalization and recycling events[10]. These cargos are transported via an intricate network of actin, microtubules, and possibly intermediate filaments tracks[8]. Studies based on immunofluorescence staining of end-binding protein 1 (EB1), which accumulates at the growing microtubule plus ends, suggest that in astrocytes bundles of microtubules radiate out from the perinucleus and extend their plus end towards the periphery[11]. However, a comprehensive examination of the organization and polarity of microtubules and other cytoskeletal elements using live-cell imaging is still lacking. While many of the mechanisms underlying the dynamics of organelles and membrane proteins have been extensively studied in neurons and other cell types, cargo motility in astrocytes is less well understood. Most of our current knowledge about changes in protein and organelle distribution in astrocytes is based on traditional antibody-based labeling of fixed preparation, which precludes precise spatial and temporal examination of cargo dynamics[7,12].

Here, we describe a method to label membrane proteins and organelles for live imaging in high purity primary mouse astrocyte cultures. Using this protocol, we provide examples in which we track the dynamic localization of green fluorescent protein (GFP)-tagged membrane proteins in transfected astrocytes, including the gap junction protein connexin 43 (Cx43-GFP) and the excitatory amino acid transporter 1 (EAAT1-GFP).

We also describe the use of a fluorescent acidotropic probe to visualize acidic organelles and follow their trafficking dynamics in live astrocytes. Finally, we demonstrate how to analyze the time-lapse data to extract and evaluate transport parameters for individual cargos.

Protocol

All animal procedures were performed with the approval of the University of North Carolina at Chapel Hill Animal Care and Use Committee (IACUC).

1. Brain dissection and culture of primary mouse astrocytes

NOTE: The following protocol was adapted from published methods, which follows the original procedure developed by McCarthy and deVellis[13,14,15]. Mixed cell cultures of McCarthy/deVellis (MD) astrocytes are prepared from postnatal day 2−4 (P2−P4) mouse cortices, treated with an anti-mitotic factor, and purified to yield the final enriched astrocyte culture. Four cortices from mouse pups of either sex are sufficient to generate one T75 tissue culture flask culture.

1. Coat the bottom of T75 flasks (100% angled neck access, 0.22 µm hydrophobic vented filter cap) with poly-D-lysine (1 mg/mL in 0.1 M Tris buffer, pH 8.5) and incubate at 37 °C for 24 h prior to start of dissection.
2. Before beginning the dissection procedure, warm 30 mL of astrocyte culture media (Dulbecco's modified Eagle's medium [DMEM] high glucose, 10% heat-inactivated fetal bovine serum, 1% penicillin/streptomycin) at 37 °C and thaw a 5 mL aliquot of 2.5% trypsin on ice. Prepare two dissecting dishes (60 mm diameter) on ice filled with 6 mL of Hank's balanced salt solution (HBSS) without Ca^{2+} or Mg^{2+}.
3. Disinfect all surgical tools (fine tip tweezers, dissecting scissors, Vannas scissors straight, Graefe forceps with curved tips) in 70% ethanol prior to and in between each dissection.
4. Spray the head and neck of the P2−P4 mouse pups with 70% ethanol before quickly euthanizing them by decapitation with surgical scissors. Perform a posterior to anterior midline incision along the scalp to expose the skull. Carefully cut the skull from the neck to the nose.
5. Perform two additional lateral incisions superior to the eyes. Using fine tip tweezers gently flip the skull flaps to the side. Remove the brain and place it in the first dissecting dish filled with ice-cold HBSS without Ca^{2+} or Mg^{2+}. Keep the dish on ice and continue harvesting the rest of the brains.
   NOTE: Perform the remainder of the dissection procedure under a dissecting scope.
6. Remove the olfactory bulbs using Vannas scissors or fine tweezers (**Figure 1Ai**). With the curved tip forceps at the intersection of the transverse and interhemispheric fissures, gently insert a second pair of curved tip forceps between the cortex and diencephalon, slowly opening the forceps to separate the cerebral hemispheres from the rest of the brain (**Figure 1Aii,Aiii**). Remove the unwanted tissue (**Figure 1Aiv**).
7. For each cortical hemisphere, carefully remove the meninges with fine tip tweezers. Optionally, remove the hippocampus from the cortices. Transfer the dissected mouse cortices into a second dish filled with ice-cold HBSS without Ca^{2+} or Mg^{2+} and keep it on ice while dissecting the remaining brains.
   NOTE: Conduct the next steps under aseptic conditions in a laminar flow hood.
8. Cut the dissected cortices into small pieces (approximately 2−4 mm) using sterile sharp surgical scissors or a scalpel. Transfer the dissected tissue to a 50 mL conical tube containing enzyme solution (22.5 mL HBSS without Ca^{2+} or Mg^{2+}, 2.5 mL 2.5% trypsin). Incubate at 37 °C for 30 min with gentle inversion every 10 min.
9. Collect the digested tissue by centrifugation at 300 x *g* for 5 min and remove the enzyme solution by decantation (do not use a vacuum aspirator). Add 10 mL of astrocyte culture media and dissociate the tissue into single cells by pipetting the solution 20−30x using a 10 mL serological pipette.
10. Filter the cell suspension through a 70 µm cell strainer to minimize cell clumps and undigested tissue. Collect the filtrate in a clean 50 mL conical tube and adjust the total volume to 20 mL with astrocyte culture media. At this point, evaluate the efficiency of the cortical dissociation by mixing 10 µL of the cell suspension with 10 µL of trypan blue and counting cells with a hemocytometer.
    NOTE: **One preparation from four P2−P4 mouse cortices yields 10−15 x 10^6 single cells.**
11. Aspirate the poly-D-lysine coating solution from the T75 culture flasks and wash twice with sterile water. Plate the 20 mL cell suspension and incubate at 37 °C and 5% CO_2.

2. Purification and maintenance of astrocyte cultures

NOTE: Perform all media changes under aseptic conditions in a laminar flow hood using sterile filtered (0.22 µm filter membrane) astrocyte media warmed to 37 °C.

1. Replace the cell media 48 h after plating (day in vitro 2, DIV2).
2. At DIV5, replace the media with fresh astrocyte culture media supplemented with 10 µM cytosine arabinoside (AraC).
   NOTE: This step facilitates the removal of contaminant cells, including fibroblasts and other glial cells. **It is important to treat the cultures with AraC no longer than 48 h as longer incubation times will reduce astrocyte viability**.
3. At DIV7, change media to astrocyte culture media without AraC and start to check the culture confluency daily. Once cells have reached 80% confluence, coat two-T75 flasks for each unpurified astrocyte culture flask with poly-D-lysine and incubate at 37 °C for at least 8 h to overnight.
4. The following day, begin the astrocyte purification by shaking the culture flasks at 180 rpm for 30 min in a 37 °C orbital shaking incubator. Remove the media and replace it with fresh astrocyte culture media. Shake cells at 240 rpm for 6 h in a 37 °C orbital shaking incubator. Prewarm 1x phosphate-buffered saline (PBS), astrocyte culture media, and 0.25% trypsin-EDTA to 37 °C 20−30 min before the end of the shaking period.
   NOTE: **CO_2 incubation is not required during the shaking steps.** If desired, the media collected after the 30-min and 6-h shaking steps may be used to culture microglia and oligodendrocytes, respectively. AraC treatment of the mixed culture will, however, reduce the abundance of the other glial cells.

5. Remove the culture flasks from the shaker and immediately replace the media with 10 mL of warm 1x PBS per flask. Remove PBS and add 3 mL of 0.25% trypsin-EDTA per flask. Incubate at 37 °C and 5% CO_2, checking every 5 min for detachment.
6. Once cells have detached from the flask, stop trypsinization by adding 10 mL of astrocyte culture media. Transfer detached astrocytes to a 50 mL conical tube and pellet cells by centrifugation at 300 x *g* for 5 min. Aspirate supernatant and re-suspend the cells in 40 mL of astrocyte culture media.
7. Wash the poly-D-lysine-coated T75 flasks twice with sterile water and plate 20 mL of the purified astrocyte suspension. Return to the 37 °C and 5% CO_2 incubator. Change the astrocyte culture media every two days for an additional 10 days until astrocytes mature.
   NOTE: Each T75 flask of purified astrocytes should be sufficient to produce 2 new T75 flasks with 3 x 10^5 cells each at plating.
8. Repeat steps 2.5−2.7 for subsequent passes or to plate astrocytes for microscopy.
   NOTE: The purity of the astrocyte cultures after the addition of AraC and following purification can be assessed qualitatively through brightfield microscopy, or more precisely by quantifying the percentage of glial fibrillary acid protein (GFAP)-positive cells per field of view in fluorescent images (**Figure 1B,C**).

3. Transfection of fluorescently tagged plasmids

1. The day prior to transfection or labeling, seed astrocytes at desired density for imaging 24−48 h post-transfection. A recommended density for 24-well plates or 14 mm glass bottom wells is 2 x 10^4 cells/well.
   NOTE: This protocol is optimized for transfection of astrocytes plated on 12 mm glass coverslips on 24-well plates or 14 mm glass bottom wells using a lipofection-based method. Reagents should be scaled depending on the size of the culture dish in which the astrocytes are growing.
2. Dilute the lipofection reagent (**Table of Materials**) in reduced-serum media (**Table of Materials**). To optimize the ratio of lipofection reagent to DNA, test a range of adequate dilutions. For example, if using the reagent employed in this protocol (**Table of Materials**), dilute 2, 3, 4, and 5 µL of the lipofection reagent in 50 µL of reduced-serum media.
3. Dilute 5 µg of high purity DNA in 250 µL of reduced-serum media. Add 5 µL of lipofection enhancer reagent (**Table of Materials**). Combine the tube containing the lipofection reagent with an equal volume of the DNA-lipofection enhancer mix. Mix by pipetting and incubate at room temperature (RT) for 15 min.
4. Remove astrocyte culture media and add transfection mix (step 3.3) to cells dropwise. After a 6-h incubation at 37 °C and 5% CO_2, replace the transfection complex with an appropriate volume of astrocyte culture media (2 mL for 14 mm glass bottom dishes). Incubate for an additional 24−72 h before proceeding to the image acquisition. Closely monitor the duration of the incubation step to achieve the best balance between protein expression and cell viability.

4. Labeling of late endosomes/lysosomes using fluorescent probes

NOTE: Some cargos can be labeled using fluorescent dyes with high affinity for cargo-specific proteins. The following example permits the labelling of late endosomes/lysosomes with a fluorescent acidotropic probe.

1. Dilute the lysosomal-labeling probe (**Table of Materials**) in 200 µL of astrocyte culture media to a working concentration of 1 µM and apply to astrocytes from step 3.1 at a density of 2 x 10^4 cells/well. Incubate for 30 min at 37 °C.
2. Wash the cells once with warm astrocyte culture media and replace with imaging media (**Table of Materials**). Proceed to live imaging immediately.

5. Image acquisition using a time-lapse imaging system

NOTE: Time-lapse live imaging should be done using a fluorescence microscope equipped with a high-speed camera, definite focus, incubation chamber, and a 40x oil objective with a high numeric aperture (e.g., Plan-Apochromat 1.4NA). A variety of acquisition software is available for time-lapse imaging. Selection of the microscopy system and acquisition software should be based on their availability and suitability for the goals of the particular study. Some general guidelines are provided below.

1. Place the culture chamber or dish in the proper adaptor on the microscope stage. Using epifluorescence light, select the cell(s) that express fluorescent proteins or probe to record. Adjust the fluorescent sample illumination to visualize the selected cell(s) using the digital camera. Avoid using high illumination that might cause photobleaching and phototoxicity. Adjust focus and zoom.
2. Acquire single Z-stack time-lapse series at a frequency of 1 frame every 2 s for time intervals ranging between 300 s and 500 s using the zoom and definite focus functions.
   NOTE: Trafficking dynamics (velocity, frequency of motion, etc.) will vary depending on the protein of interest, thus, the time course of acquisition may require adjustment. For instance, mitochondria are less motile than lysosomes and exhibit frequent pauses. In this instance, it is more appropriate to adjust the acquisition parameters to 1 frame every 5 s for 800 s.
3. Save time-lapse images and export them as AVI or TIFF stack files.

6. Image analysis

NOTE: Image analysis was performed using the KymoToolBox plugin for ImageJ/Fiji[16]. Detailed step-by-step written instructions are available online[17]. The following abbreviated steps should be sufficient to create the kymographs and extract the particle transport parameters.

1. Open time-lapse image sequence in ImageJ/Fiji software. Import images from the **File** menu as AVI or TIFF stack files. Convert the images to 8-bit or 16-bit by selecting one of these image types using the **Type** tool from the **Image** menu. If working with RGB files, split channels using the **Split Channel** tool available under the **Color** feature in the **Image** menu.
2. To generate a kymograph (representation in position and time of particle trajectories), draw each track in which particles are moving by tracing a line along the trajectories of the particles using the **segmented line** tool. To correctly assign directionality of the movement, draw the

polyline using the same desired directional convention for all movies so that the polarity is consistent within and across all cells being studied. For instance, draw the polyline from the center of the cell towards the periphery or vice versa. Adjust the line width to match the thickness of the track by double clicking the **Line** tool.

3. Run the **Draw Kymo** macro of the KymoToolBox plugin using a line width of 10. A prompt asking to calibrate the image in time (number of frames, frame rate) and space (x,y resolution) will appear. Once calibrated, the kymographs are generated and can be saved as TIFF files for data presentation or further particle analysis.
4. Assign particle trajectories by manually tracking each particle in the kymograph using the **segmented line** tool for the full duration of the acquisition. Record each particle trajectory as a region of interest (ROI) using the **ROI manager** tool found in the **Analyze/Tools** menu. Save all ROIs per each time-lapse video for further analysis.
   NOTE: It is critical to assign the correct trajectory for individual particles on the kymograph to achieve the most accurate calculation of transport parameters.
   1. Run the **Analyze Kymo** macro of the KymoToolBox plugin. A window will open asking to define the "outward" direction of particle motion (from left to right or vice versa) from the drop-down menu. This selection depends on the position of the fluorescent cargos imaged relative to the nucleus or the cell periphery, as established in step 6.2. For instance, if the nucleus is positioned to the left of the cargos, and the polyline in step 6.2 was drawn away from the nucleus, define the outward particle motion as "from left to right".
   2. Define the limit speed (minimum speed at which a cargo is considered motile) in the **Analyze Kymo** window. For cargos that move at fast intracellular transport speeds, 0.1 µm/second is an appropriate choice. Modify this value to adjust the software's sensitivity to each cargo of interest. Adjust the line width to match the thickness of each particle trajectory.
   3. Select the **Log all data** and **Log extrapolated coordinates** options in the **Analyze kymo** window. This will calculate various cargo transport parameters, including mean speed, inward speed, outward speed, cumulative distance traveled, distance traveled in either the inward or outward direction, number of switches for each particle, percentage of time moving in each direction or paused, etc. Data calculated for individual tracks are then pooled per kymograph and saved in text files specific to each image.
      NOTE: The **Show Colored Kymo** option of **Analyze Kymo** macro generates a color-coded overlay of the path over the original kymograph. Particles traveling outward are colored in green, inward in red, and stationary particles in blue. The **Report Coordinates on Original Stack** option of the **Analyze Kymo** macro generates a color-coded overlay of the extrapolated object's position on the original time-lapse video and kymograph.

Representative Results

The protocol for establishing primary mouse MD astrocytes outlined above should yield reproducible, high quality cultures. Although cultures initially contain a mix of astrocytes, fibroblasts, and other glial cells, including microglia and oligodendrocytes (**Figure 1Bi,Biv**; red arrowheads), the addition of AraC to the mixed culture between DIV5-DIV7 minimizes the proliferation of these contaminant cells. The combined AraC treatment and shaking-based purification strategy enriches the purity of the astrocyte cultures (**Figure 1Bii**) over traditional protocols that only include the purification steps (**Figure 1Bv**; blue arrowheads)[13]. The expected morphology and composition (assessed by GFAP and 4',6-diamidino-2-phenylindole [DAPI] staining) of the purified astrocyte cultures treated with AraC or left untreated is shown in **Figure 1Biii,Bvi**. Quantification of the percentage of the $GFAP^+$ cells per field of view (ratio of number of cells with GFAP staining to total number of cells identified by DAPI staining) shows an increase of over 27% in purity with AraC supplementation (**Figure 1C**). This high-purity mouse astrocyte culture is suitable for evaluation of RNA and protein expression, cell morphology, and other functional assays.

We used lipofection-based transfection to express GFP-tagged versions of the gap junction protein Cx43 and the EAAT1 transporter in murine astrocytes. This methodology allows transient expression of proteins at levels that are optimal for live cell imaging without causing toxicity or affecting astrocyte viability (**Figure 2A,E**). Similarly, the use of a fluorescent probe permitted rapid and efficient labelling of acidic endo-lysosomal organelles (**Figure 2I**) to track their dynamics in astrocytes.

Figure 2 shows representative results of the analyses of cargo dynamics in astrocytes transiently transfected with EAAT1-GFP, Cx43-GFP, or labeled with a selective dye that recognizes acidic endolysosomal vesicles. Each of these cargos appeared as a fluorescent punctum decorating the perinuclear region, cytosol, and processes of astrocytes (**Figure 2A,E,I,** left panels). The time-lapse data was used to generate kymographs that track cargo motion in time and space (**Figure 2A,E,I, right panels**). In these kymographs, anterograde and retrograde movement of the indicated cargo is represented by trajectories with negative (green lines) and positive (red lines) slopes, respectively. Stationary vesicles are shown as vertical trajectories (blue lines). Kymograph analysis revealed that the three types of cargo analyzed undergo bidirectional transport with occasional fast, processive runs in both directions. Furthermore, quantification of the flux of a cargo through an area of the astrocyte (red box) revealed differences in the percentage of motile particles among cargos. For example, while 70% of EAAT1-GFP puncta are stationary (**Figure 2B**), less than 20% of Cx43-GFP (**Figure 2F**) and 45% of probe-labeled endolysosomal cargos (**Figure 2J**) are non-motile. These differences in motility among cargos are likely representative of their normal, baseline motility in the region of the astrocyte where the movies were acquired.

The precise mapping of the change in X-Y position along the full time scale for each particle obtained from the kymograph can also be used to evaluate other motion parameters, such as cargo velocity (**Figure 2C,G,K**) and run length (distance traveled) (**Figure 2D,H,L**). Motion parameters can be further analyzed for individual cargos to determine changes in directionality of movement (anterograde vs retrograde motion) as well as reversals in particle direction of motion, number of pauses, etc. The results from these types of analyses can provide meaningful quantitative information regarding changes in the cellular distribution of organelles and membrane proteins in astrocytes under basal or abnormal conditions in the intra- and extracellular environment.

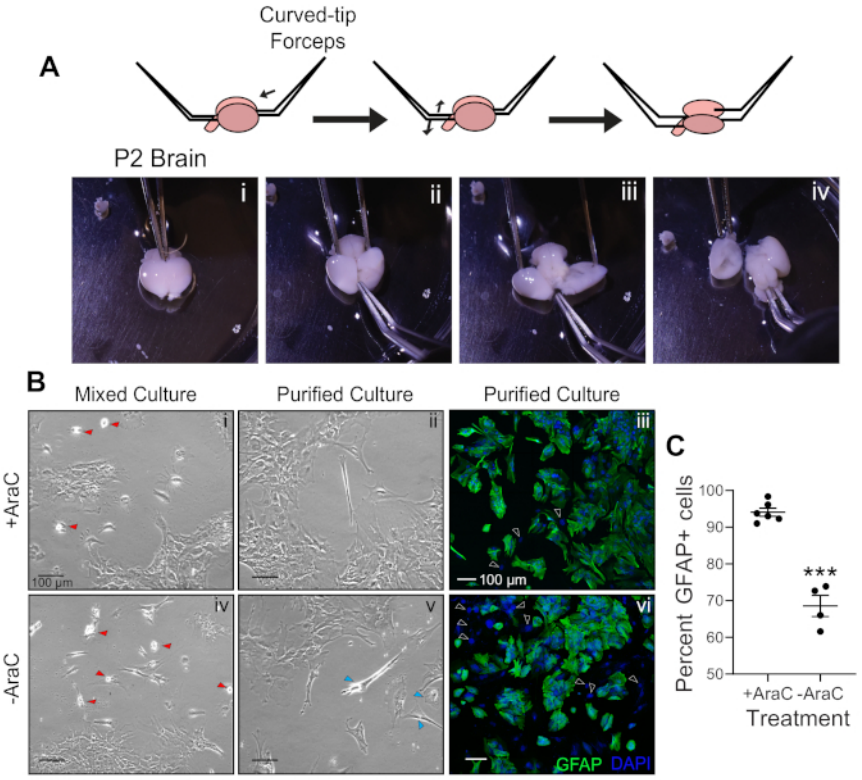

Figure 1: Establishment of primary mouse astrocyte cultures.
(**A**) Steps required for dissection of P2−P4 mouse brains. (**B**) (**i,iv**) Brightfield images of mixed glial cultures treated (**i**) and non-treated (**iv**) with AraC. Red arrowheads indicate contaminant microglia. (**ii,v**) Images of purified astrocyte cultures treated (**ii**) and non-treated (**v**) with AraC. Blue arrowheads indicate contaminant oligodendrocytes. (**iii,vi**) Confocal images of purified astrocyte cultures treated (**iii**) and non-treated (**vi**) with AraC. Green shows GFAP staining and DAPI (blue) labels all nuclei. (**C**) Percentage of GFAP-positive cells. Data represents mean ± SEM. ***p < 0.001, unpaired t-test. Please click here to view a larger version of this figure.

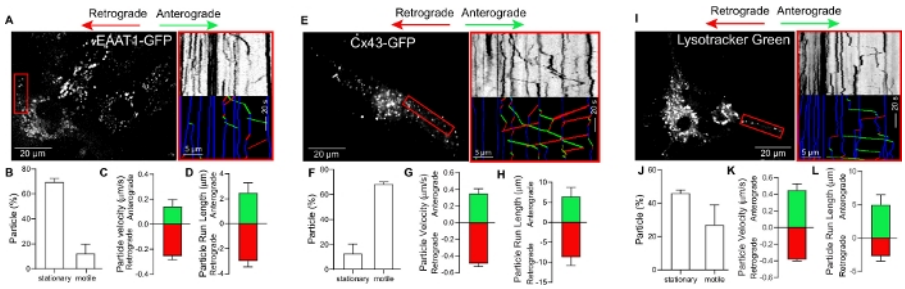

Figure 2: Quantitative analyses of cargo dynamics in astrocytes.
(**A,E,I**) Left panels: Astrocytes expressing EAAT1-GFP (A), Cx43-GFP (**E**) or treated with a probe that labels late endosomes and lysosomes (**I**). Red boxes indicate regions used to analyze particle dynamics. Right panels: Original and color-coded kymographs showing trajectories for the indicated cargos. Red lines represent retrograde-moving cargos, green lines anterograde-moving cargos, and blue lines non-motile cargos. (**B,F,J**) Percentage of stationary and motile particles. (**C,G,K**) Quantification of anterograde and retrograde velocity and (**D,H,L**) run length. Data represents mean ± SEM. Please click here to view a larger version of this figure.

Discussion

Here, we describe an experimental approach to express, visualize, and track fluorescently tagged organelles and membrane proteins of interest using time-lapse video microscopy in high-purity primary mouse cortical MD astrocytes. We also outline a methodology for measuring particle dynamics. Direct visualization of protein and organelle dynamics in primary astrocytes provides a powerful tool to study the regulation of intracellular transport in these cells in vitro.

The methodology for establishing mouse MD astrocyte cultures described above combines steps from other published protocols[13,14,15], which results in both a simpler method and in higher purity and quality cultures. The combination of AraC[15] treatment and shaking-based purification[13,14] can yield astrocyte cultures with a purity as high as 98% (assessed by the ratio of $GFAP^+$ cells total cells), which in our example results in a 27% increase in purity over cultures subjected to the purification steps only (**Figure 1B,C**). The high purity cultures of mouse astrocytes obtained with this method is similar to the values reported for rat astrocyte cultures (assessed by enzymatic assays and electron

microscopy) by McCarthy and deVellis[14]. However, the McCarthy/deVellis method, which does not include AraC treatment, requires a longer shaking step (15−18 h) and two additional rounds of purification[14].

In our example, we show that this protocol is sufficiently sensitive to capture differences in motility among various membrane proteins and organelles in astrocytes, which are likely representative of their individual intracellular itineraries and cellular function. Although our example demonstrates the utility of this protocol at basal conditions, this methodology can be easily adapted to measure transport parameters within a broad range of research questions. For example, similar protocols with minor modifications could be used to characterize transport events in astrocytes in vitro in response to intra- or extracellular environment, such as cellular damage, toxicity, pathogenic mutations, synaptic activity (in mixed cultures of neurons and astrocytes), etc. Likewise, co-expression and visualization of multiple cargos or organelles, each individually tagged with different fluorophores, can also be used to assess dynamic changes in co-localization and complex formation, transient interactions between organelles, and endocytic and membrane recycling transport events.

The success of the methodology presented here primarily relies on the ability to obtain high-quality astrocyte cultures and in the efficient labeling of cargo(s) of interest. When utilizing this procedure for live imaging, it is important to closely monitor fluorescent expression to determine the optimal post-transfection incubation time. On average, we found that for the cargos analyzed a 24-h incubation period results in good signal intensity for live imaging acquisition. Prolonged incubation of transfected astrocytes can result in high expression of fluorescently tagged proteins, which can induce protein aggregation, thus changing cargo localization and dynamics, and diminishing the health of the cultures. Astrocytes are very vulnerable to physical damage and changes in the culture environment, which can lead to induction of transcriptional and cellular responses, including reactivity. Therefore, it is critical to reduce the time intervals between washing steps, and to minimize exposure of the cultures to air and to significant changes in temperature or light intensity over the incubation and acquisition periods.

In summary, the methods presented here can be used to evaluate and quantify dynamic changes in protein and organelle localization in astrocytes. They provide valuable tools that permit the examination of changes in astrocytic responses under physiological and pathological conditions.

Disclosures

The authors have nothing to disclose.

Acknowledgments

DNL was supported by the University of North Carolina at Chapel Hill (UNC) School of Medicine as a Simmons Scholar. TWR was supported by UNC PREP Grant R25 GM089569. Work using the UNC Neuroscience Center Microscopy Core Facility was supported, in part, by funding from the NIH-NINDS Neuroscience Center Support Grant P30 NS045892 and the NIH-NICHD Intellectual and Developmental Disabilities Research Center Support Grant U54 HD079124.

References

1. Barres, B. A. The mystery and magic of glia: a perspective on their roles in health and disease. *Neuron.* **60** (3), 430-440 (2008).
2. Araque, A., Parpura, V., Sanzgiri, R. P., Haydon, P. G. Tripartite synapses: Glia, the unacknowledged partner. *Trends in Neurosciences.* **22** (5), 208-215 (1999).
3. Zuchero, J. B., Barres, B. A. Glia in mammalian development and disease. *Development.* **142** (22), 3805-3809 (2015).
4. Allaman, I., Bélanger, M., Magistretti, P. J. Astrocyte-neuron metabolic relationships: for better and for worse. *Trends in Neurosciences.* **34** (2), 76-87 (2011).
5. Chung, W. S., Barres, B. A. The role of glial cells in synapse elimination. *Current Opinion in Neurobiology.* **22** (3), 438-445 (2012).
6. Chung, W. S., Allen, N. J., Eroglu, C. Astrocytes Control Synapse Formation, Function, and Elimination. *Cold Spring Harbor Perspectives in Biology.* **7** (9), a020370 (2015).
7. Shin, J. W. et al. Distribution of glutamate transporter GLAST in membranes of cultured astrocytes in the presence of glutamate transport substrates and ATP. *Neurochemistry Research.* **34** (10), 1758-1766 (2009).
8. Potokar, M. et al. Cytoskeleton and vesicle mobility in astrocytes. *Traffic.* **8** (1), 12-20 (2007).
9. Potokar, M. et al. Regulation of AQP4 surface expression via vesicle mobility in astrocytes. *Glia.* **61** (6), 917-928 (2013).
10. Potokar, M., Lacovich, V., Chowdhury, H. H., Kreft, M., Zorec, R. Rab4 and Rab5 GTPase are required for directional mobility of endocytic vesicles in astrocytes. *Glia.* **60** (4), 594-604 (2012).
11. Chiu, C. T. et al. HYS-32-Induced Microtubule Catastrophes in Rat Astrocytes Involves the PI3K-GSK3beta Signaling Pathway. *PLoS ONE.* **10** (5), e0126217 (2015).
12. Basu, R., Bose, A., Thomas, D., Das Sarma, J. Microtubule-assisted altered trafficking of astrocytic gap junction protein connexin 43 is associated with depletion of connexin 47 during mouse hepatitis virus infection. *Journal of Biological Chemistry.* **292** (36), 14747-14763 (2017).
13. Schildge, S., Bohrer, C., Beck, K., Schachtrup, C. Isolation and culture of mouse cortical astrocytes. *Journal of Visual Experiments.* (71), e50079 (2013).
14. McCarthy, K. D., de Vellis, J. Preparation of separate astroglial and oligodendroglial cell cultures from rat cerebral tissue. *The Journal of Cell Biology.* **85** (3), 890-902 (1980).
15. Tedeschi, B., Barrett, J. N., Keane, R. W. Astrocytes produce interferon that enhances the expression of H-2 antigens on a subpopulation of brain cells. *The Journal of Cell Biology.* **102** (6), 2244-2253 (1986).
16. Zala, D. et al. Vesicular glycolysis provides on-board energy for fast axonal transport. *Cell.* **152** (3), 479-491 (2013).
17. Cordelières, F. P. *IJ_KymoToolBox*. [software]. https://github.com/fabricecordelieres/IJ_KymoToolBox (2016).

